

Iterative Frequency Domain Equalization and Carrier Synchronization for Multi-Resolution Constellations

P. Pedrosa, R. Dinis, and F. Nunes

Abstract—Broadband broadcast and multicast wireless systems usually employ OFDM modulations (Orthogonal Frequency Division Multiplexing) combined with non-uniform hierarchical constellations. However, these schemes are very prone to non-linear distortion effects and have high carrier synchronization requirements. SC-FDE (Single-Carrier with Frequency-Domain Equalization) is an attractive alternative for OFDM, especially when an efficient power amplification is intended. In this paper we consider the use of SC-FDE schemes combined with non-uniform hierarchical constellations in broadband broadcast and multicast wireless systems. We study the impact of residual CFO (Carrier Frequency Offset) on the performance of multi-resolution schemes and we propose iterative frequency domain receivers with joint detection and carrier synchronization to cope with residual CFO estimation errors (a coarse CFO estimation and compensation is assumed before the equalization procedure). Our results show that while a very high carrier synchronization accuracy is required for the least protected bits, the most protected bits are relatively robust to the CFO. By employing the proposed receiver we increase significantly the robustness to residual CFO estimation errors.

Index Terms—Carrier frequency offset, multi-resolution transmission, non-uniform hierarchical QAM, single carrier with frequency-domain equalization.

I. INTRODUCTION

IN BROADCAST and multicast wireless systems we transmit the same information to several users which can have substantially different propagation conditions. It can be shown [1] that it is possible to exchange some of the capacity of the good communication links to the poor ones. A very simple method to improve the efficiency of the network is to use non-uniform hierarchical constellations which are able to provide bit streams with different error protections [2]. This means that we have two or more classes of bits with different error protections. A given user can attempt to demodulate only the more protected bits or also the other bits that carry the additional information, depending on the channel conditions; we can also have low-cost terminals only able to receive the most protected bits. An application of these techniques is in the transmission of coded voice or video signals, where different

error protections may be associated to different resolutions [2], [3].

An important drawback of non-uniform signal constellations is that they are very sensitive to residual interference. This can be the residual ISI (Inter-Symbol Interference) at the output of a practical equalizer that does not invert completely the channel effects (e.g., an equalizer optimized under the MMSE (Minimum Squared Mean Error) [4]). Since phase errors lead to significant performance degradation, these constellations are also very sensitive to carrier frequency errors.

For broadband broadcast and multicast wireless systems the time-dispersion effects associated to the multipath propagation can be severe. In this case, conventional time-domain equalization schemes are not practical. Alternative techniques employing block transmission with appropriate cyclic extensions and employing FDE (Frequency-Domain Equalization) techniques have been shown to be suitable for high data rate transmission over severely time-dispersive channels without requiring complex receivers. For this reason, OFDM (Orthogonal Frequency Division Multiplexing) modulations [5] are usually selected for these systems [6], [7]. However, the OFDM signals have high envelope fluctuations and a high PMEPR (Peak-to-Mean Envelope Power Ratio) leading to amplification difficulties. For this reason, several techniques have been proposed for reducing the envelope fluctuations of OFDM signals (see [8] and references within), although the transmitted signals still have higher envelope fluctuations than SC (Single-Carrier) signals based on similar constellations. Moreover, since the subcarrier spacing is a very small fraction of the transmission bandwidth, the carrier synchronization requirements are also much higher for OFDM modulations.

An alternative approach based on the same block transmission principle is SC modulations (Single-Carrier) combined with FDE (also denoted SC-FDE) [9]. When compared with OFDM, SC-FDE has the advantage of reduced envelope fluctuations and higher robustness to carrier frequency errors (contrarily to OFDM schemes, where frequency errors lead to ICI [10]–[12], for SC-FDE the CFO induces a rotation in the constellation that grows linearly along the block). The performance of SC-FDE can be further improved if the traditional linear FDE is replaced by an IB-DFE (Iterative Block-Decision Feedback Equalizer) [13]. An IB-DFE receiver with joint post-equalization carrier frequency synchronization was proposed in [14], which can be regarded as a modified turbo equalization scheme where, for each iteration, we perform DD (Decision-directed) CFO (Carrier Frequency Offset) estimation, allowing high robustness against residual CFO.

Earlier IB-DFE implementations considered hard-decisions (weighted by the blockwise reliability) in the feedback loop. To improve the performance and allow truly turbo FDE implementations, IB-DFE schemes with soft decisions were proposed

Manuscript received June 10, 2008; revised August 19, 2010; accepted August 19, 2010. Date of publication September 23, 2010; date of current version November 19, 2010. This work was supported in part by the FCT—Fundação para a Ciência e Tecnologia under pluriannual funding, by the ADCOD project PTDC/EEA - TEL/099973/2008, by the U-BOAT project PTDC/EEA - TEL/67066/2006, and by the Ph.D. Grant SFRH / BD / 40265 / 2007.

P. Pedrosa and F. Nunes are with the Instituto de Telecomunicações, and also with the Instituto Superior Técnico, Universidade Técnica de Lisboa, 1040-001 Lisboa, Portugal (e-mail: ppedrosa@lx.it.pt; nunes@lx.it.pt).

R. Dinis is with the Instituto de Telecomunicações, 1040-001 Lisboa, Portugal and also with the Faculdade de Ciências e Tecnologia, Universidade Nova de Lisboa, 2829-516 Caparica, Portugal (e-mail: rdinis@lx.it.pt).

Color versions of one or more of the figures in this paper are available online at <http://ieeexplore.ieee.org>.

Digital Object Identifier 10.1109/TBC.2010.2073251

[15]–[17] usually only for QPSK constellations. The extension for larger constellations leads to difficulties on the computation of the reliability of each block, as well as problems on the computation of the average symbol values conditioned to the FDE and the channel decoder output. Notably, carrier synchronization for QAM differs from carrier synchronization for QPSK specially for large constellations which are particularly sensitive to CFO. In [18] SC-FDE schemes with IB-DFE receivers were considered and a general method for the computation of the receiver parameters for any constellation was proposed. The approach in [18] relies on an analytical characterization of the mapping rule where the constellation symbols are written as a linear function of the transmitted bits. This method is then employed in both uniform and non-uniform hierarchical QAM constellations.

There are two major contributions of this paper. First, we consider the use of SC-FDE schemes combined with multi-resolution for broadband broadcast and multicast wireless systems, in opposition to most works on multi-resolution that consider OFDM implementations. Second, we study the impact of residual CFO (Carrier Frequency Offset) on the performance of multi-resolution schemes. We assume that a coarse CFO estimation and compensation is made before the equalization procedure, but the coarse CFO estimate can have a significant error leading to a residual CFO. To cope with this residual CFO, we present and evaluate an iterative frequency domain receiver with joint detection and carrier synchronization.

This paper is organized in following manner: Section II pertains to the description of the system, with subsections dedicated to the mapping rules, the receiver scheme and the computation of the parameters of the receiver; Section III reports the performance results; and finally Section IV concludes this paper.

II. SYSTEM DESCRIPTION

A. Mapping Rules

Assume the transmitted symbols s_n belong to a given alphabet \mathcal{G} (i.e. a given constellation) with dimension $M = \#\mathcal{G}$ and are selected according to the corresponding bits $\beta_n^{(m)}$, $m = 1, 2, \dots, \mu$ ($\mu = \log_2(M)$). i.e., $s_n = f(b_n^{(1)}, b_n^{(2)}, \dots, b_n^{(\mu)})$, with $b_n^{(m)} = 2\beta_n^{(m)} - 1$. We assume that $\beta_n^{(m)}$ is the m th bit associated to the n th symbol and $b_n^{(m)}$ is the corresponding polar representation, i.e., $\beta_n^{(m)} = 0$ or 1 and $b_n^{(m)} = -1$ or $+1$, respectively.

For 4-PAM constellations and Gray mapping it can be shown that [18]

$$s_n = d_1 b_n^{(2)} + d_2 b_n^{(1)} b_n^{(2)}, \quad (1)$$

If $k = d_2/d_1 = 0.5$ we have that (1) is uniform whereas if $0 < k < 0.5$ then (1) is non-uniform and truly hierarchical [2]. For 8-PAM constellations and Gray mapping we have

$$s_n = d_1 b_n^{(3)} + d_2 b_n^{(3)} b_n^{(2)} + d_3 b_n^{(3)} b_n^{(2)} b_n^{(1)}. \quad (2)$$

Again, if $k = d_2/d_1 = d_3/d_2 = 0.5$ (2) is uniform¹ whereas if $0 < k < 0.5$ (2) is non-uniform and truly hierarchical. Clearly, our PAM constellations can be written as the sum of several

binary polar constellations with amplitudes d_1, d_2 , etc, and k is a parameter that characterizes the “non-uniform” degree of the constellations.

It should be mentioned that hierarchical QAM constellations have higher PMEPR than QPSK constellations. However, their PMEPR is lower than for uniform QAM and for systems with very different error protections ($k \ll 0.5$) the PMEPR can be close to the one with QPSK. Moreover, the PMEPR is much lower for SC-FDE than for OFDM with the same constellation (hierarchical or not).

If the transmitted symbols are selected from a QAM constellation under a Gray mapping rule the M -QAM constellation is written as the sum of two PAM constellations each with dimension \sqrt{M} , one for the in-phase (real) component and other for the quadrature (imaginary) component. Therefore, the corresponding mapping is straightforward: half of the bits are used to define the in-phase component and the other half is used to define the quadrature component. Considering a square constellation we obtain for 16-QAM

$$s_n = d_1 b_n^{(2)} + d_2 b_n^{(1)} b_n^{(2)} + j \left(d_1 b_n^{(4)} + d_2 b_n^{(3)} b_n^{(4)} \right), \quad (3)$$

and for 64-QAM

$$s_n = d_1 b_n^{(3)} + d_2 b_n^{(3)} b_n^{(2)} + d_3 b_n^{(3)} b_n^{(2)} b_n^{(1)} + j \left(d_1 b_n^{(6)} + d_2 b_n^{(6)} b_n^{(5)} + d_3 b_n^{(6)} b_n^{(5)} b_n^{(4)} \right) \quad (4)$$

B. IB-DFE Receiver With Joint Carrier Synchronization

Considering Fig. 1, the received time domain block, $\{y'_n; n = 0, 1, \dots, N-1\}$, is passed to the frequency domain by a DFT operation, leading to the block $\{Y'_k; k = 0, 1, \dots, N-1\}$, with

$$Y'_k = S'_k H_k + N_k, \quad (5)$$

where H_k and N_k denote the channel transfer function and the channel noise, respectively, for the k th subchannel. The block of frequency-domain symbols $\{S'_k; k = 0, 1, \dots, N-1\}$ is the DFT of the transmitted time-domain block, $\{s'_n; n = 0, 1, \dots, N-1\}$, with

$$s'_n = s_n \exp \left(j 2\pi \frac{\Delta f n T}{N} \right), \quad (6)$$

where s_n denotes the n th data symbol to be transmitted, selected from a given constellation (e.g. a QAM or a PSK constellation), T is the duration of the block, and Δf is the CFO.

For a given iteration i , the frequency-domain samples at the output of the FDE are given by

$$\tilde{S}_k^{(i)} = F_k^{(i)} Y'_k - B_k^{(i)} \tilde{S}_k^{(i-1)}, \quad (7)$$

where $\{F_k^{(i)}; k = 0, 1, \dots, N-1\}$ are the feedforward coefficients and $\{B_k^{(i)}; k = 0, 1, \dots, N-1\}$ are the feedback coefficients. $\{\tilde{S}_k^{(i-1)}; k = 0, 1, \dots, N-1\}$ denotes the DFT of the block of the time-domain average symbol values associated to the previous iteration, $\{\tilde{s}_n^{(i-1)}; n = 0, 1, \dots, N-1\}$.

The DD estimation of the carrier frequency offset can be implemented using

$$\widehat{\Delta f} = \frac{N}{2\pi M T} \arg\{\xi\} \quad (8)$$

¹Actually we could have two different ratios $k_1 = d_2/d_1$ and $k_2 = d_3/d_2$.

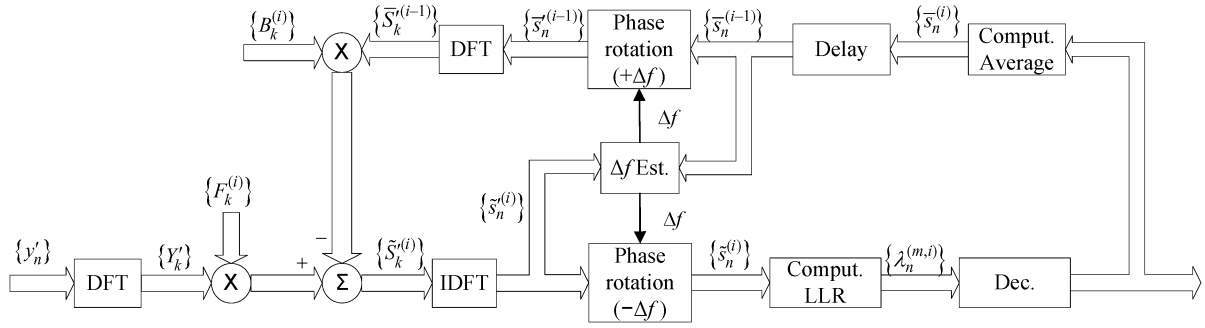


Fig. 1. Proposed receiver for joint equalization and carrier synchronization with soft decisions.

where ξ is given by

$$\xi = \sum_{n=0}^{N-M-1} \tilde{s}'_{n+M} \tilde{s}_n^* \tilde{s}_{n+M} \bar{s}_n, \quad (9)$$

and where the optimal value for M is $\lfloor (2/3)N \rfloor$ [14].

It can be shown that the optimum feedback coefficients are [19], [20]²

$$B_k^{(i)} = F_k^{(i)} H_k - 1 \quad (10)$$

and the feedforward coefficients are given by

$$F_k^{(i)} = \frac{\check{F}_k^{(i)}}{\gamma^{(i)}} \quad (11)$$

with

$$\check{F}_k^{(i)} = \frac{H_k^*}{\alpha + (1 - (\rho^{(i-1)})^2) |H_k|^2}, \quad (12)$$

where $\alpha = E[|N_k|^2]/E[|S_k|^2]$. In (11) we have

$$\gamma^{(i)} = \frac{1}{N} \sum_{k=0}^{N-1} \check{F}_k^{(i)} H_k \quad (13)$$

and the correlation factor $\rho^{(i-1)}$ in (12) is defined as

$$\rho^{(i-1)} = \frac{E[\hat{s}_n^{(i-1)} s_n^*]}{E[|s_n|^2]}, \quad (14)$$

where the block $\{\hat{s}_n^{(i-1)}; n = 0, 1, \dots, N-1\}$ denotes the data estimates associated to the previous iteration, i.e., the hard-decisions associated to the time-domain block at the output of the FDE, $\{\tilde{s}_n^{(i)}; n = 0, 1, \dots, N-1\} = \text{IDFT}\{\tilde{S}_k^{(i)}; k = 0, 1, \dots, N-1\}$.

C. Computation of the Average Values and the Correlation Factor

To determine the average symbol values conditioned to the FDE output, \bar{s}_n , we need to obtain the average bit values conditioned to the FDE output, $\bar{b}_n^{(m)}$. These are related to the corresponding log-likelihood ratio as follows:

²contrarily to [19] and [20], we are considering normalized equalizers, i.e., $\sum_{k=0}^{N-1} F_k^{(i)} H_k = 1$.

$$\bar{b}_n^{(m)} = \tanh\left(\frac{\lambda_n^{(m)}}{2}\right) \quad (15)$$

using mapping rules (1)–(4) with (15) we obtain \bar{s}_n .

The log-likelihood ratio of the m th bit of the n th transmitted symbol is given by [18]

$$\begin{aligned} \lambda_n^{(m)} &= \log\left(\frac{\Pr(\beta_n^{(m)} = 1)}{\Pr(\beta_n^{(m)} = 0)}\right) \\ &= \log\left(\frac{\sum_{s \in \Psi_1^{(m)}} \exp\left(-\frac{|s_n - s|^2}{2\sigma^2}\right)}{\sum_{s \in \Psi_0^{(m)}} \exp\left(-\frac{|s_n - s|^2}{2\sigma^2}\right)}\right) \end{aligned} \quad (16)$$

where $\Psi_1^{(m)}$ and $\Psi_0^{(m)}$ are the subsets of \mathcal{G} where $\beta_n^{(m)} = 1$ or 0, respectively (clearly $\Psi_1^{(m)} \cup \Psi_0^{(m)} = \mathcal{G}$ and $\Psi_1^{(m)} \cap \Psi_0^{(m)} = \emptyset$).

The reliability of the estimates to be used in the feedback loop are given by

$$\rho = \frac{1}{2N} \sum_{n=0}^N (\rho_n^I + \rho_n^Q), \quad (17)$$

where ρ_n^I and ρ_n^Q can be regarded as the reliabilities associated to the real and imaginary parts of the n th symbol, respectively. It can be shown that for 16-QAM we have [18]

$$\rho_n^I = \frac{d_1^2 |\bar{b}_n^{(2)}| + d_2^2 |\bar{b}_n^{(2)} \bar{b}_n^{(1)}|}{d_1^2 + d_2^2} \quad (18)$$

and

$$\rho_n^Q = \frac{d_1^2 |\bar{b}_n^{(4)}| + d_2^2 |\bar{b}_n^{(4)} \bar{b}_n^{(3)}|}{d_1^2 + d_2^2} \quad (19)$$

and for 64-QAM we obtain

$$\rho_n^I = \frac{d_1^2 |\bar{b}_n^{(3)}| + d_2^2 |\bar{b}_n^{(3)} \bar{b}_n^{(2)}| + d_3^2 |\bar{b}_n^{(3)} \bar{b}_n^{(2)} \bar{b}_n^{(1)}|}{d_1^2 + d_2^2 + d_3^2} \quad (20)$$

and

$$\rho_n^Q = \frac{d_1^2 |\bar{b}_n^{(6)}| + d_2^2 |\bar{b}_n^{(6)} \bar{b}_n^{(5)}| + d_3^2 |\bar{b}_n^{(6)} \bar{b}_n^{(5)} \bar{b}_n^{(4)}|}{d_1^2 + d_2^2 + d_3^2}. \quad (21)$$

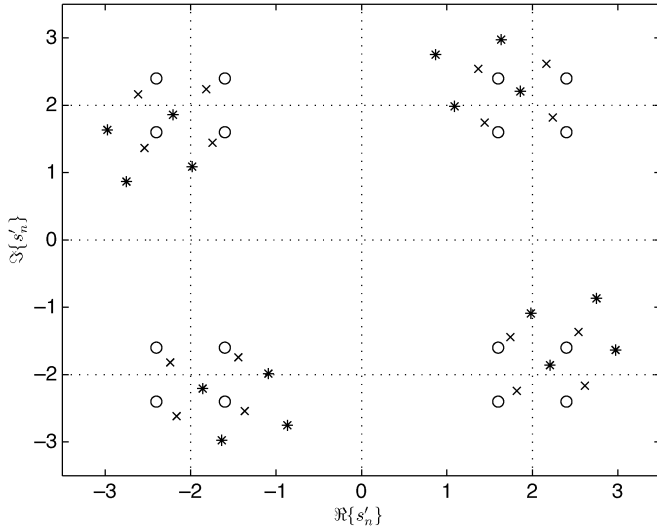


Fig. 2. Hierarchical 16-QAM constellation for phase rotations $\theta = 0, 0.0942$ and 0.1885 rad, denoted by “o”, “x”, and “*”, respectively. The decision thresholds are indicated by the dotted line.

For the first iteration, $\rho_n^I = \rho_n^Q = 0$ and $\bar{s}_n = 0$. Note that (17) allows to compute the correlation factor ρ without the explicit knowledge of the transmitted symbols s_n as with (14).

III. PERFORMANCE RESULTS

Fig. 2 shows the impact of different phase rotations θ on a hierarchical 16-QAM constellation with $k = d_2/d_1 = 0.2$. We considered $\theta = 0, 0.0942$ and 0.1885 rad, corresponding to the maximum phase rotation (i.e., the phase rotation at the end of the block) for $\Delta fT = 0, 0.015$ and 0.03 , respectively. From this figure it is clear that for large phase rotation (i.e., high residual CFO) we can have errors in the LPB (that are associated to the smaller sub constellations) even without noise while the MPB still have some noise robustness.

In the following we present a set of experimental results. We consider SC-FDE modulations with blocks of $N = 512$ “useful” modulation symbols, plus an appropriate cyclic prefix. The symbol duration is 7.8 ns, corresponding to blocks where the useful part has duration equal to $4 \mu\text{s}$. Additionally, we consider linear power amplification and perfect channel estimation. The propagation channel is characterized by the power delay profile type C for HIPERLAN/2 (High PERFORMANCE Local Area Network) [21], with uncorrelated Rayleigh fading on different paths (similar results could be obtained for other severely time dispersive channel models with rich multipath propagation). For the hierarchical modulations we considered $k = 0.3$.

In Fig. 3 we can see the BER as a function of the CFO normalized to the symbol duration ΔfT for hierarchical 16-QAM constellations. The derivation of the analytical expression of the BER as a function of the CFO is straightforward but lengthy, therefore the results depicted in Fig. 3 were obtained through Monte Carlo simulations. The derivation of the analytical expression of the BER as a function of the CFO was done in [14] for QPSK constellations. The CFO creates a phase rotation in each constellation symbol that grows linearly within the block.

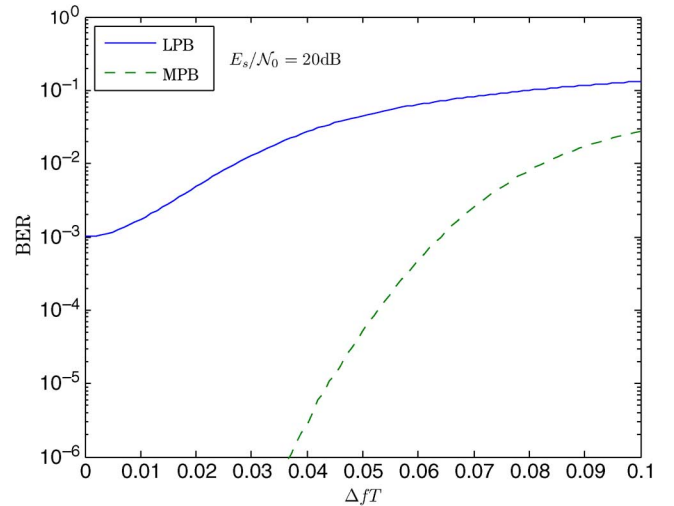


Fig. 3. Plot of BER versus the CFO normalized to the symbol duration ΔfT for hierarchical 16-QAM.

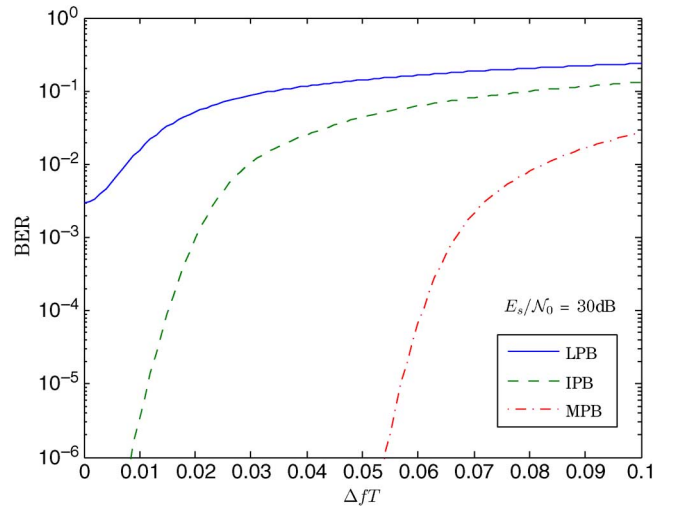


Fig. 4. Plot of BER versus the CFO normalized to the symbol duration ΔfT for hierarchical 64-QAM.

Therefore, computing the BER with CFO can be done by computing the BER for each phase rotation and averaging it over the block. The extension of the analytical expression of the BER as a function of the CFO for non-uniform QAM constellations is straightforward but tedious, since the expression of the BER with a given phase error can be very long. This happens because we need to take into account all possible combinations of the interference between the in-phase and quadrature components.

By inspecting Fig. 3 one can see that the MPB is more robust to the presence of CFO than the LPB.

In Fig. 4 we plot the BER as a function of the CFO normalized to the symbol duration ΔfT for hierarchical 64-QAM constellations. Represented in the graphic are the curves for MPB, IPB (Intermediate Protected Bits), and LPB. We see that hierarchical constellations provide different degrees of protection to the presence of CFO with the MPB being the most resistant to the presence of CFO.

In Fig. 5 we depict the performance of the IB-DFE receiver with a hierarchical 16-QAM constellation in the presence of a

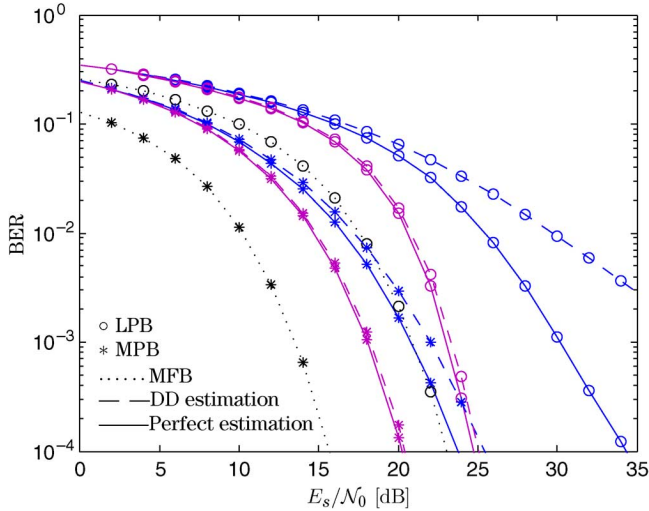


Fig. 5. BER performance for hierarchical 16-QAM constellations with a CFO normalized to the symbol duration $\Delta fT = 0.03$.

CFO normalized to the symbol duration $\Delta fT = 0.03$. The curves are depicted in the figure for perfect estimation, corresponding to $\hat{\Delta f} = \Delta f$, and DD estimation, corresponding to the use of (8) and (9). Additionally, we also plot the MFB (see Appendix). Those curves were traced for the LPB and MPB. For each of the transmission modes, LPB or MPB, the curves are traced for the first and fifth iteration. In order to distinguish the first iteration from the fifth iteration, one must notice that the fifth iteration corresponds to the best results for each transmission modes, i.e., to the curves that are nearer the MFB. Also shown in the figure is the trade off between power and error protection. We see that, for the first iteration, in order to the MPB transmission mode to achieve the same BER as the LPB transmission mode the MPB transmission mode has to dispense approximately more 10 dB, in the high power/low error region. For the fifth iteration this difference reduces to approximately 5 dB, for the same region. Also noteworthy is the improvement verified with the iterative process for the MPB transmission mode: at the fifth iteration in the low error region we can see an improvement of approximately 10 dB, which is very close to the MFB. On the other hand, for the LPB transmission mode although the improvement is less noticeable one still has 5 dB of improvement. With respect to the synchronization procedure, we see that the DD estimation and subsequent compensation of the CFO produces results that are very close to those obtained with perfect synchronization. On the other hand, for the first iteration, one does not have any CFO compensation, therefore the curve corresponding to the DD estimation is in reality the curve of an uncompensated transmission.

In Fig. 6 the performance of the IB-DFE receiver with joint CFO estimation is presented for a hierarchical 64-QAM constellation with a CFO normalized to the symbol duration $\Delta fT = 0.015$. The curves that were traced are the same as for Fig. 5 with the additional curves of the IPB. Again, the curves of the fifth iteration are those nearer the corresponding MFB. By inspecting the figure we can see that for the same BER the power demand increases with the protection of the bits, so for the MPB transmission mode has to use approximately more 10 dB than

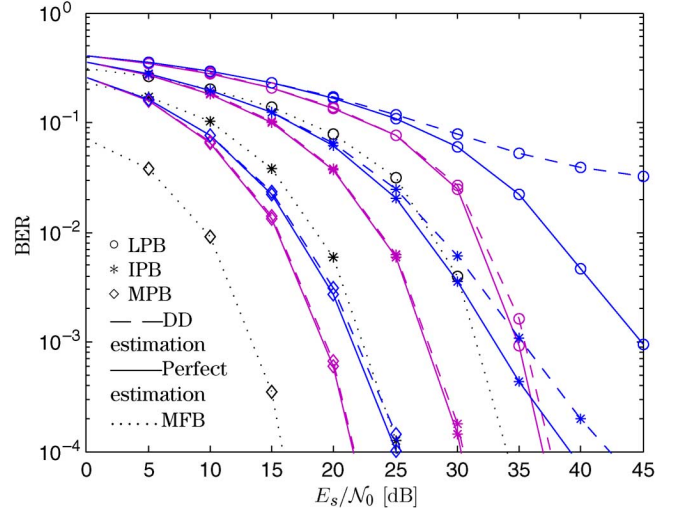


Fig. 6. BER performance for hierarchical 64-QAM constellations with a CFO normalized to the symbol duration $\Delta fT = 0.015$.

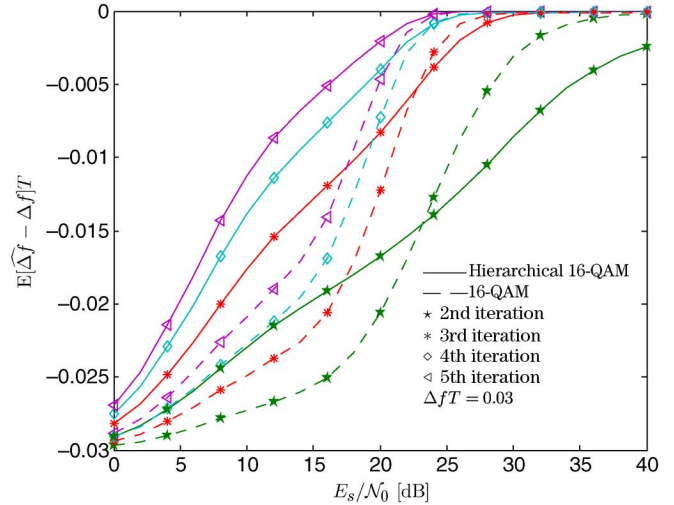


Fig. 7. Comparison between the bias of the CFO estimates for uniform and hierarchical 16-QAM, with a CFO normalized to the symbol duration $\Delta fT = 0.03$.

for the IPB, and for the IPB we need to dispense approximately more 10 dB than for the LBP. This for the low error region. With respect to the synchronization procedure, we can see that, as with Fig. 5 the DD estimation procedure produces results that are very close to those obtained with perfect synchronization.

Fig. 7 compares the bias of the CFO estimates obtained using 16-QAM and hierarchical 16-QAM. By inspecting the figure we see that, for the second iteration, in the region of low to moderate E_s/N_0 the hierarchical modulation has a lower absolute value for the bias whereas for higher values of E_s/N_0 the QAM modulation presents the best performance. This suggests that hierarchical QAM modulations offer better protection to CFO than QAM modulations, when operating in the low to moderate region of E_s/N_0 . For iterations $i = 3, 4, 5$ a similar behavior can be observed.

Fig. 8 compares the bias of the CFO estimates obtained using 64-QAM and hierarchical 64-QAM. By inspecting the figure we reach similar conclusions to those respecting Fig. 7: for low

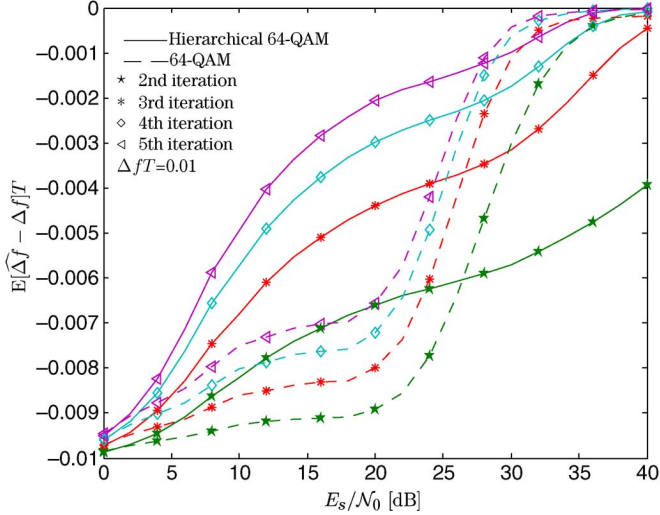


Fig. 8. Comparison between the bias of the CFO estimates for uniform and hierarchical 64-QAM, with a CFO normalized to the symbol duration $\Delta fT = 0.01$.

to moderate E_s/N_0 , hierarchical modulations offer increased protection to CFO when compared to QAM modulations.

IV. CONCLUSIONS

In this paper we considered the use of SC-FDE schemes combined with non-uniform hierarchical constellations for broadband broadcast and multicast wireless systems. The impact of CFO (Carrier Frequency Offset) on the performance was studied, showing that while a very high carrier synchronization accuracy is required for the least protected bits, the most protected bits are relatively robust to the CFO.

To improve the performance in the presence of carrier synchronization errors, we proposed and evaluated an iterative frequency-domain receiver with joint equalization and estimation of residual CFO.

Our results show that while a very high carrier synchronization accuracy is required for the LPB (Least Protected Bits), the MPB (Most Protected Bits) are relatively robust to the CFO. It is also shown that the proposed receivers can have excellent performances, allowing good BERs with moderate frequency offsets and severely time dispersive channels.

APPENDIX

The bit error probabilities for generalized hierarchical QAM transmissions over AWGN channel with Gray coding are given in [22], [23]. Here we use the leading term approximation of the bit error probability to compute the MFB for hierarchical 16-QAM and 64-QAM.

For hierarchical 16-QAM, the leading term approximation for the MPB is given by the leading term approximation of the probability of error of the most significant bit (msb), i.e., $b_n^{(1)}$

$$P_e^{\text{msb}}(\gamma_s) \approx \frac{1}{2} \mathcal{Q} \left(\sqrt{\gamma_s (d_1 - d_2)^2 / (d_1^2 + d_2^2)} \right), \quad (22)$$

i.e.,

$$P_e^{\text{MPB}}(\gamma_s) = P_e^{\text{msb}}(\gamma_s), \quad (23)$$

where $\gamma_s = E_s/N_0$. On the other hand, the probability of error of the LPB is given by

$$P_e^{\text{LPB}}(\gamma_s) = \frac{1}{2} (P_e^{\text{msb}}(\gamma_s) + P_e^{\text{lsb}}(\gamma_s)), \quad (24)$$

where the leading term approximation of the least significant bit (lsb) is given by

$$P_e^{\text{lsb}}(\gamma_s) \approx \mathcal{Q} \left(\sqrt{\gamma_s d_2^2 / (d_1^2 + d_2^2)} \right). \quad (25)$$

Thus, the MFB for the MPB is given by

$$\text{MFB}^{\text{MPB}} = \frac{1}{2} \mathcal{Q} \left(\sqrt{\frac{E_s}{N_0} \frac{1}{N} \sum_{k=0}^{N-1} |H_k|^2 \frac{(d_1 - d_2)^2}{(d_1^2 + d_2^2)}} \right), \quad (26)$$

whereas the MFB for the LPB is given by

$$\begin{aligned} \text{MFB}^{\text{LPB}} &= \frac{1}{4} \mathcal{Q} \left(\sqrt{\frac{E_s}{N_0} \frac{1}{N} \sum_{k=0}^{N-1} |H_k|^2 \frac{(d_1 - d_2)^2}{(d_1^2 + d_2^2)}} \right) \\ &+ \frac{1}{2} \mathcal{Q} \left(\sqrt{\frac{E_s}{N_0} \frac{1}{N} \sum_{k=0}^{N-1} |H_k|^2 \frac{d_2^2}{(d_1^2 + d_2^2)}} \right). \quad (27) \end{aligned}$$

For hierarchical 64-QAM the probability of error of bit $b_n^{(1)}$ is given by

$$P_e^{\text{msb}}(\gamma_s) \approx \frac{1}{4} \mathcal{Q} \left(\sqrt{\gamma_s (d_1 - d_2 - d_3)^2 / (d_1^2 + d_2^2 + d_3^2)} \right) \quad (28)$$

and for the intermediate significant bit, $b_n^{(2)}$, it is given by

$$\begin{aligned} P_e^{\text{isb}}(\gamma_s) &\approx \frac{1}{2} \left(\mathcal{Q} \left(\sqrt{\gamma_s (d_2 + d_3)^2 / (d_1^2 + d_2^2 + d_3^2)} \right) \right. \\ &\left. + \mathcal{Q} \left(\sqrt{\gamma_s (d_2 - d_3)^2 / (d_1^2 + d_2^2 + d_3^2)} \right) \right) \quad (29) \end{aligned}$$

and for $b_n^{(3)}$ it is given by

$$P_e^{\text{lsb}}(\gamma_s) \approx \mathcal{Q} \left(\sqrt{\gamma_s d_3^2 / (d_1^2 + d_2^2 + d_3^2)} \right). \quad (30)$$

The bit error probability for the MPB is given by (23), where P_e^{msb} is given by (28). As for the bit error probability concerning the IPB we have

$$P_e^{\text{IPB}}(\gamma_s) = \frac{1}{2} (P_e^{\text{msb}}(\gamma_s) + P_e^{\text{isb}}(\gamma_s)). \quad (31)$$

On the other hand the bit error probability for the LPB is given by,

$$P_e^{\text{LPB}}(\gamma_s) = \frac{1}{3} (P_e^{\text{msb}}(\gamma_s) + P_e^{\text{isb}}(\gamma_s) + P_e^{\text{lsb}}(\gamma_s)). \quad (32)$$

The MFB for the MPB is given by

$$\text{MFB}^{\text{MPB}} = \frac{1}{4} \mathcal{Q} \left(\sqrt{\frac{E_s}{\mathcal{N}_0} \frac{1}{N} \sum_{k=0}^{N-1} |H_k|^2 \frac{(d_1 - d_2 - d_3)^2}{(d_1^2 + d_2^2 + d_3^2)}} \right), \quad (33)$$

whereas the MFB for the IPB is given by

$$\begin{aligned} \text{MFB}^{\text{IPB}} &= \frac{1}{8} \mathcal{Q} \left(\sqrt{\frac{E_s}{\mathcal{N}_0} \frac{1}{N} \sum_{k=0}^{N-1} |H_k|^2 \frac{(d_1 - d_2 - d_3)^2}{(d_1^2 + d_2^2 + d_3^2)}} \right) \\ &+ \frac{1}{4} \mathcal{Q} \left(\sqrt{\frac{E_s}{\mathcal{N}_0} \frac{1}{N} \sum_{k=0}^{N-1} |H_k|^2 \frac{(d_2 + d_3)^2}{(d_1^2 + d_2^2 + d_3^2)}} \right) \\ &+ \frac{1}{4} \mathcal{Q} \left(\sqrt{\frac{E_s}{\mathcal{N}_0} \frac{1}{N} \sum_{k=0}^{N-1} |H_k|^2 \frac{(d_2 - d_3)^2}{(d_1^2 + d_2^2 + d_3^2)}} \right), \end{aligned} \quad (34)$$

whereas the MFB for the LPB is given by

$$\begin{aligned} \text{MFB}^{\text{LPB}} &= \frac{1}{12} \mathcal{Q} \left(\sqrt{\frac{E_s}{\mathcal{N}_0} \frac{1}{N} \sum_{k=0}^{N-1} |H_k|^2 \frac{(d_1 - d_2 - d_3)^2}{(d_1^2 + d_2^2 + d_3^2)}} \right) \\ &+ \frac{1}{6} \mathcal{Q} \left(\sqrt{\frac{E_s}{\mathcal{N}_0} \frac{1}{N} \sum_{k=0}^{N-1} |H_k|^2 \frac{(d_2 + d_3)^2}{(d_1^2 + d_2^2 + d_3^2)}} \right) \\ &+ \frac{1}{6} \mathcal{Q} \left(\sqrt{\frac{E_s}{\mathcal{N}_0} \frac{1}{N} \sum_{k=0}^{N-1} |H_k|^2 \frac{(d_2 - d_3)^2}{(d_1^2 + d_2^2 + d_3^2)}} \right) \\ &+ \frac{1}{3} \mathcal{Q} \left(\sqrt{\frac{E_s}{\mathcal{N}_0} \frac{1}{N} \sum_{k=0}^{N-1} |H_k|^2 \frac{d_3^2}{(d_1^2 + d_2^2 + d_3^2)}} \right) \end{aligned} \quad (35)$$

ACKNOWLEDGMENT

The authors would like to thank the anonymous reviewers for their valuable comments.

REFERENCES

- [1] T. Cover, "Broadcast channels," *IEEE Trans. Inf. Theory*, vol. 18, no. 1, pp. 2–14, Jan. 1972.
- [2] H. Jiang and P. Wilford, "A hierarchical modulation for upgrading digital broadcast systems," *IEEE Trans. Broadcast.*, vol. 51, no. 2, pp. 223–229, Jun. 2005.
- [3] K. Ramchandran, A. Ortega, K. Uz, and M. Vetterli, "Multiresolution broadcast for digital HDTV using joint source/channel coding," *IEEE J. Sel. Areas in Commun.*, vol. 11, no. 1, pp. 6–23, Jan. 1993.
- [4] J. Proakis, *Digital Communications*, 3rd ed. New York: McGraw-Hill, 1995, ch. 10, pp. 607–617.
- [5] L. Cimini, Jr., "Analysis and simulation of a digital mobile channel using orthogonal frequency division multiplexing," *IEEE Trans. Commun.*, vol. 33, pp. 400–411, Jul. 1985.
- [6] Z.-W. Zheng, Z.-X. Yang, C.-Y. Pan, and Y.-S. Zhu, "Effects of nonlinear distortion and imperfect parameters estimation on the performance of OFDM-based DTTB systems," *IEEE Trans. Broadcast.*, vol. 51, no. 2, pp. 237–243, Jun. 2005.
- [7] H.-C. Wu, "Analysis and characterization of intercarrier and interblock interferences for wireless mobile OFDM systems," *IEEE Trans. Broadcast.*, vol. 52, no. 2, pp. 203–210, Jun. 2006.
- [8] R. Dinis and A. Gusmão, "A class of nonlinear signal-processing schemes for bandwidth-efficient OFDM transmission with low envelope fluctuation," *IEEE Trans. Commun.*, vol. 52, no. 11, pp. 2009–2018, Nov. 2004.
- [9] H. Sari, G. Karam, and I. Jeanclaude, "An analysis of orthogonal frequency-multiplexing for mobile radio applications," in *Proc. IEEE Veh. Technol. Conf.*, Stockholm, Jun. 1994, pp. 1635–1639.
- [10] H.-C. Wu and Y. Wu, "Distributive pilot arrangement based on modified m-sequences for OFDM intercarrier interference estimation," *IEEE Trans. Wireless Commun.*, vol. 6, no. 5, pp. 1605–1609, May 2007.
- [11] X. Huang, H.-C. Wu, and Y. Wu, "Novel pilot-free adaptive modulation for wireless OFDM systems," *IEEE Trans. Veh. Technol.*, vol. 57, no. 6, pp. 3863–3867, Nov. 2008.
- [12] H.-C. Wu and Y. Wu, "A new ICI matrices estimation scheme using Hadamard sequence for OFDM systems," *IEEE Trans. Broadcast.*, vol. 51, no. 3, pp. 305–314, Sep. 2005.
- [13] N. Benvenuto, R. Dinis, D. Falconer, and S. Tomasin, "Single carrier modulation with nonlinear frequency domain equalization: An idea whose time has come—again," *Proc. IEEE*, vol. 98, no. 1, pp. 69–96, Jan. 2010.
- [14] T. Araújo and R. Dinis, "Iterative equalization and carrier synchronization for single-carrier transmission over severe time-dispersive channels," in *Proc. IEEE Global Commun. Conf.*, Dallas, Texas, Nov./Dec. 29–3, 2004, vol. 5, pp. 3103–3107.
- [15] N. Benvenuto and S. Tomasin, "Iterative design and detection of a DFE in the frequency domain," *IEEE Trans. Commun.*, vol. 53, no. 11, pp. 1867–1875, Nov. 2005.
- [16] A. Gusmão, P. Torres, R. Dinis, and N. Esteves, "A class of iterative FDE techniques for reduced-CP SC-based block transmission," in *Int. Symp. Turbo Codes*, Apr. 2006.
- [17] A. Gusmão, P. Torres, R. Dinis, and N. Esteves, *A turbo FDE technique for reduced-CP SC-based block transmission*, vol. 55, no. 1, pp. 16–20, Jan. 2007.
- [18] R. Dinis, P. Montezuma, N. Souto, and J. Silva, "Iterative frequency-domain equalization for general constellations," in *Proc. IEEE Sarnoff Symp. 2010*, Princeton, USA, Apr. 2010, pp. 1–5.
- [19] R. Dinis, A. Gusmão, and N. Esteves, "On broadband block transmission over strongly frequency-selective fading channels," in *IEEE Wireless*, Calgary, Canada, Jul. 2003.
- [20] N. Benvenuto and S. Tomasin, "Block iterative DFE for single carrier modulation," *IEEE Electron. Lett.*, vol. 39, no. 19, pp. 1144–1145, Sep. 2002.
- [21] *Channel models for HIPERLAN/2 in different indoor scenarios*, ETSI EP BRAN 3ERI085B, ETSI, Mar. 1998, pp. 1–8.
- [22] P. Vitthaladevuni and M.-S. Alouini, "BER computation of generalized QAM constellations," in *IEEE Global Telecommun. Conf.*, 2001, vol. 1, pp. 632–636.
- [23] P. Vitthaladevuni and M.-S. Alouini, "A closed-form expression for the exact BER of generalized PAM and QAM constellations," *IEEE Trans. Commun.*, vol. 52, no. 5, pp. 698–700, May 2004.